Available online at www.sciencedirect.com
SCIENCE DIRECT®
Journal of Organometallic Chemistry 690 (2005) 2339–2350
Journal of Organometallic Chemistry
www.elsevier.com/locate/jorganchem

Alkyl-rhodium transition state stabilities as a tool to predict regio- and stereoselectivity in the hydroformylation of chiral substrates

Giuliano Alagona *, Caterina Ghio

CNR-IPCF, Istituto per i Processi Chimico-Fisici, Molecular Modeling Laboratory, Via Moruzzi 1, I-56124 Pisa, Italy

Received 1 December 2004; revised 21 December 2004; accepted 21 December 2004
Available online 14 April 2005

Abstract

A theoretical investigation on the stability of the alkyl rhodium transition states as the key-step determining the regio- and diastereoselective outcomes of the hydroformylation reaction with an unmodified rhodium catalyst ($H–Rh(CO)_3$) has been carried out. The results obtained employing effective core potentials for Rh in the LANL2DZ valence basis set, with the other atoms described at the B3P86/6-31G* level, have been compared to those computed with B3LYP/SBK(d), using effective core potentials for Rh and main group atoms. A number of contaminations between those levels or additional basis functions have also been used. The substrates considered are three related chiral olefins, namely (1-vinyloxy-ethyl)-benzene (**1**), (1-methyl-but-3-enyl)-benzene (**2**), and (1-methyl-allyl)-benzene (**3**). The structural features of the various possible complexes, which show a second chiral center at the inner olefin carbon upon complexation, do not present major changes among the various computational descriptions for each substrate. Significant differences in relative stabilities of the lowest energy transition states can be detected in the case of the ethereal substrate (**1**), whereas for both chiral alkenes (**2** and **3**) only very small energy gaps have been computed. In the case of **1** and **2**, a quantitative agreement with available experimental results is obtained at the B3P86/6-31G* level, that should allow the prediction of regio- and stereoselectivity for chiral olefins not already screened. The B3LYP/SBK(d) values are comparable to the B3P86/6-31G* ones, although in the case of vinylether (**1**) the B3LYP/SBK(d) regioisomeric ratio turns out to be critical.

Keywords: Regioselectivity; Diastereoselectivity; Unmodified rhodium catalysts; Theoretical investigation

1. Introduction

Hydroformylation of alkenes, one of the largest industrial catalytic processes, is used for the production of aldehydes [1], which can conveniently be converted to alcohols [2]. Though discovered many years ago [3], this reaction is still being studied both experimentally [1,4] and theoretically [5] to elucidate its mechanism. The hydroformylation reaction makes use of a number of homogeneous transition metal complexes as catalysts. The most common are low-valent cobalt and rhodium [2,4a,6] complexes, albeit complexes based on Pt, Ru, Ir and Pd are used in asymmetric hydroformylation [7]. Since the economical value of the final product is linked to the nature of the aldehyde (linear, L, or branched, B), it is very important to control the reaction regioselectivity. In the case of branched aldehydes with chiral centers, such as those displayed in Scheme 1, the reaction diastereoselectivity is to be considered as well. Obviously, analogous schemes can be imagined for chiral unsaturated substrates without any separator (no X group), one of them taken also into account in this investigation.

* Corresponding author. Tel.: +39 050 3152450; fax: +39 050 3152442.
E-mail address: G.Alagona@ipcf.cnr.it (G. Alagona).

0022-328X/$ - see front matter © 2005 Elsevier B.V. All rights reserved.
doi:10.1016/j.jorganchem.2004.12.038

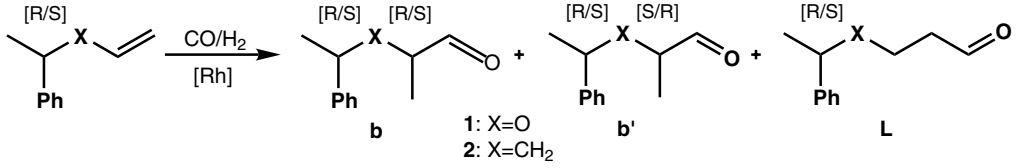

Scheme 1.

A reliable method to obtain an a priori estimate of the reaction regio- and diastereoselectivities, i.e., the regioisomeric (B:L, with B = b + b′) and diastereomeric (b:b′) ratios between the aldehydes produced, would be very helpful because of the monetary value of chiral unsaturated substrate hydroformylation and might even save a good number of experimental trials.

Of course, there are several factors affecting the reaction outcome. Among them, substrate structure and properties, reaction parameters (P, T, concentration), and nature of the catalyst (unmodified, or modified with phosphorous ligands) are those playing the most important role. The presence of phosphine ligands, mainly because of steric hindrance [5d], somewhat inhibits the activity of the catalyst imposing severe reaction conditions without a generalized improvement in selectivity, although unmodified catalysts are sometimes charged with low selectivity [1c]. However, this is not always true, as clearly shown in the case of styrene [8]. Conversely, with unmodified catalysts, such as those employed in this study, the reaction occurs under mild conditions, where other typical side processes are negligible. This allows a consistent comparison between theoretical and experimental (obtained using $[Rh_4(CO)_{12}]$ as a catalyst precursor) results, without any interference from phosphine ligands. Additionally, as much simpler models than modified catalysts, they have a heuristic function, since the hydroformylation mechanism is far from being well understood [1c]. Last, but not least, the computational complexity of the system is significantly lower.

As far as the particular reactions reported in Scheme 1 are concerned, branched aldehydes decidedly prevail over linear regioisomers when X = O and, between the possible pairs of diastereomers of the branched aldehyde, the (R,R) or (S,S) pair, i.e., b, prevails over the (R,S) or (S,R) one, i.e., b′. In contrast, when $X = CH_2$, the prevalence of one species over the other is very limited or vanishingly small [9]. Of course, different results can be obtained in the case of a diverse substrate, even in analogous experimental conditions.

The hypothesis that the regio- and diastereoselectivity of the hydroformylation reaction originate at the alkyl formation step was confirmed in our previous theoretical investigations [10] by comparison with experiments employing unmodified rhodium catalysts in mild conditions. It is worth noting that an experimental determination of the relative concentrations of isomeric alkyl rhodium intermediates (not to mention transition states) is not allowed, since they are very reactive under typical hydroformylation conditions. The experimental evidence is thus confined to the aldehyde products.

In the present investigation, the stability of the alkyl rhodium transition states for three chiral substrates at various computational levels is considered. Aim of this study is not just of assessing which of them is adequate and affordable to eventually predict the outcome of hydroformylation reactions with different olefins as substrates, but also of evaluating and analyzing their behavior. In addition the computational strategy is discussed, because even sophisticated computational descriptions miserably fail without an accurate and careful conformational analysis within each configuration.

2. Computational details

All the calculations have been carried out with the Gaussian98 system of programs [11] in the density functional theory (DFT) framework. Gradient-corrected Becke's three parameter hybrid exchange [12] and Perdew's P86 gradient-corrected correlation [13] functionals, B3P86, at the 3-21G [14] and 6-31G* [15] levels for C, O and H have been used, coupled for Rh to effective core potentials (which implicitly include some relativistic effects for the electrons near the nucleus) in the LANL2DZ [16] corresponding valence basis set. In what follows, for the sake of simplifying the notation, reference to 3-21G and 6-31G* basis sets stand for 3-21G/LANL2DZ and 6-31G*/LANL2DZ, i.e., both names include also the aforementioned Rh description without any need of mentioning it again. The 3-21G results are reported in Supplementary Material (Tables S1–S3).

Another set of calculations has been carried out using B3LYP/SBK(d), that is the gradient-corrected Becke's three parameter hybrid exchange functional, as above, and the Lee, Yang, Parr's correlation [17] functional. SBK(d) denotes the effective core potential basis set of Stevens et al. [18] (named CEP-31G in Gaussian), employed for Rh and the main group atoms, with CEP replacing, respectively, the 14 innermost core orbitals only and the *1s* orbitals, but augmented with a *d* polarization function [19]. Thus, 17 electrons for Rh are included in the valence space and treated explicitly; the associated Rh valence basis set is of quadruple and triple ζ quality for the *sp* and *d* shells, respectively, with a

(4211/4211/311) contraction pattern, while the valence basis set for the main group elements (*sp* shells) is of double ζ quality with a (31/31) contraction pattern. Conversely, for hydrogens the standard split valence 31G basis set [20] was used. The B3LYP/SBK(d) results have a slightly lower (by about 5%) computational cost than the B3P86/6-31G* ones. Calculations with a number of contaminations between the aforementioned levels and/or with additional basis functions have been carried out for comparison: they are described in detail where appropriate.

Due to the difficulty of discriminating between real vibrations and hindered rotations, only internal energies have been utilized, as implied our previous results on this kind of systems [10], although vibrational frequencies have been computed to ascertain the nature of stationary points under consideration.

2.1. Choice of model systems and definitions

The systems considered, displayed in Scheme 2, are representative of aryl/alkyl substituted vinyl ethers and hydrocarbon olefins, with significant differences in their regio- and diastereoselectivities for **1** and **2** [10b], as put forward above. As far as **3** is concerned, to the best of our knowledge, no experimental data are available thus far for hydroformylation reactions carried out on that substrate with unmodified rhodium catalysts in mild conditions, although a low regioselectivity was observed at 60 °C for allylbenzene using zwitterionic rhodium complexes as catalysts [9d]. Therefore it is interesting to collate its results to those obtained in the presence of X separators. Since a similar orientation of the substituents at the chiral center makes visual comparisons easier, the R chirality is adopted for substrate **1**, whereas the S chirality is adopted for substrates **2** and **3** because of the Cahn–Ingold–Prelog (CIP) priority rules.

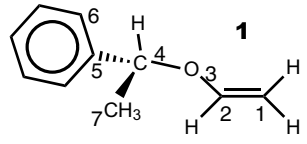

(1-vinyloxy-ethyl)-benzene

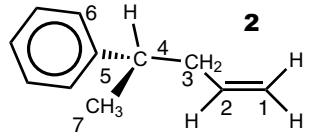

(1-methyl-but-3-enyl)-benzene

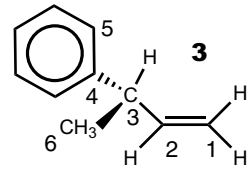

(1-methyl-allyl)-benzene

Scheme 2.

Furthermore, the chirality of the developing stereogenic center for an alkyl rhodium transition state (TS) is opposite to that obtained for the branched aldehyde product (shown in Scheme 1). This is due to the formal change of chirality at the C_2 carbon atom again occurring ought to the CIP priority rules ($Rh > O > CH_2$ and $O > CHO > CH_3$, for substrate **1** for alkyls and aldehydes, respectively; analogously there is a priority inversion for substrates **2** and **3** when CHO replaces Rh). Therefore, to avoid misunderstandings, especially in the comparison to experimental data, the branched aldehyde chirality is used everywhere, even when discussing about TS. In addition, we'll distinguish between linear TS diastereomers ℓ and ℓ' (that are theoretically possible, in contrast to what happens for the linear aldehyde product which shows a single chiral center), instead of naming L both of them. Since in this case it is impossible to refer to the linear aldehyde chirality, we use ℓ' when both chiral centers at the transition state have the same chirality, for the sake of consistency with the b/b′ definition (vide infra).

A brief reminder of regio- and diastereoselectivity formulas is reported in order to make the paper self-contained. Since the olefin insertion occurs irreversibly and without subsequent changes in the branched to linear distribution at room temperature [1,21,22], assuming a Boltzmann distribution between the two pathways, the regioselectivity can be computed from the relative energies of the B (= b + b′) and L (= $\ell + \ell'$) transition states only [23]:

$$\mathrm{B} : \mathrm{L} = k_{\mathrm{B}} : k_{\mathrm{L}} = \sum \mathrm{e}^{-\Delta G_{\mathrm{B}}^{\neq}/RT} : \sum \mathrm{e}^{-\Delta G_{\mathrm{L}}^{\neq}/RT} = \sum \mathrm{e}^{-\Delta\Delta G^{\neq}/RT} \approx \sum \mathrm{e}^{-\Delta\Delta E^{\neq}/RT}$$

as already shown in our previous articles as well [10].

For diastereoselectivity to be computed, it is necessary to consider the individual diastereomers shown in Scheme 1. Indeed, the alkyl rhodium TS can be either RS or RR (by considering the chiral reactant as R only, for the sake of simplicity). Since at the aldehyde level they correspond to RR (b) and RS (b′) branched aldehydes, respectively, the linear alkyl rhodium TS are named ℓ when their chiral centers show different chirality at TS and ℓ' (same chirality at TS). The evaluation of both diastereomeric ratios can be thus performed in close analogy to regioisomeric ratios by using the relevant relative stabilities of the diastereomeric transition states ($\Delta\Delta E^{\neq}$):

$$\mathrm{b} : \mathrm{b}' = k_{\mathrm{b}} : k_{\mathrm{b}'} = \sum \mathrm{e}^{-\Delta G^{\neq}_{\mathrm{b}}/RT} : \sum \mathrm{e}^{-\Delta G^{\neq}_{\mathrm{b}'}/RT} = \sum \mathrm{e}^{-\Delta\Delta G^{\neq}/RT} \approx \sum \mathrm{e}^{-\Delta\Delta E^{\neq}/RT},$$

$$\ell : \ell' = k_{\ell} : k_{\ell'} = \sum \mathrm{e}^{-\Delta G^{\neq}_{\ell}/RT} : \sum \mathrm{e}^{-\Delta G^{\neq}_{\ell'}/RT} = \sum \mathrm{e}^{-\Delta\Delta G^{\neq}/RT} \approx \sum \mathrm{e}^{-\Delta\Delta E^{\neq}/RT}.$$

3. Results and discussion

The main structural change along the reaction coordinate from reactants (trigonal-bipyramidal, TBP) to transition states (square-planar pyramidal, SP) occurs via the Berry pseudo-rotation mechanism [10a,24], that brings the axial ligands and two of the equatorial ones to a basal position, causing the third equatorial ligand to become apical (see Scheme 3), where schematic representations of actual ligands are also displayed.

Therefore the prominent geometrical feature of an alkyl rhodium TS concerns its SP structure: the apical ligand (one of the CO groups) is about perpendicular to the basal ligands that are in turn almost opposite with respect to rhodium in couples (CO–H and CO–vinyl C). Once the diametrically opposed basal ligands are located, the identification of the apical CO group is straightforward. Nevertheless, the presence of three identical equatorial ligands in H–Rh(CO)$_3$ may, in principle, give rise to two possible arrangements of the TS, depending on which of the ligands takes the apical position, with a very limited conformational change, but significantly different Rh–CO distances. It is worth mentioning, however, that these two arrangements are not always both locatable.

Besides the conformational freedom within the catalytic group, a number of positions of the olefin relative to it must be considered. As already stressed, a careful conformational search is to be carried out for each configuration, because of the difficulty in determining all low energy transition states. Failure of considering even one of low energy TS structures can blur the regio- and stereomeric theoretical picture, that is very sensitive to small energy changes. Therefore all possible arrangements of the olefin backbone have been optimized at the B3P86/3-21G level while keeping fixed the dihedral angles defining them to relax bad contacts, in the presence of the catalytic group. To avoid rotational transition states, minimum energy structures have been determined for tentative alkyl rhodium TS reached with the hydride about halfway between Rh and the olefin C (Rh···H = 1.65 Å, C···H = 1.6 Å). Then TS optimizations (invariably performed with the CalcFC option) have been carried out relieving also the latter constraints. Geometries of the alkyl rhodium TS have been optimized at the higher levels starting from B3P86/3-21G geometries obtained first.

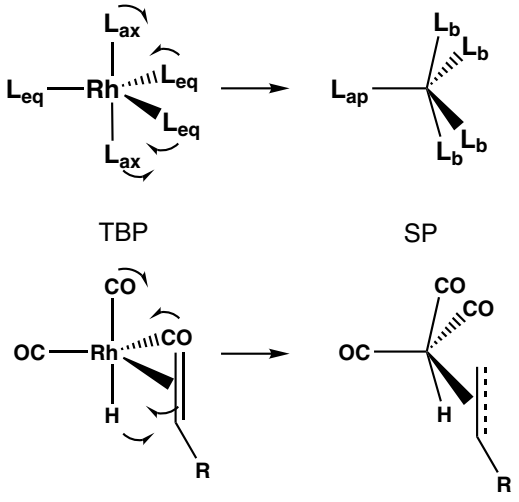

Scheme 3.

It is worth noting that the energy ordering of the various spatial arrangements is not always conserved at the distinct computational levels, identified for short with a two-character acronym. Consequently, 6d and SB subscripts stand for B3P86/6-31G* and B3LYP/SBK(d), respectively, maintaining this order when values computed with both basis sets are discussed. Some of the geometric parameters for the lowest energy alkyl rhodium TS diastereomers (b, b′, ℓ, ℓ′) of each system are reported in Supplementary Material (Tables S4, S5 and S6), respectively.

Each TS is characterized through its type (b, b′, ℓ, ℓ′) and its relative energy (ΔE, in kcal/mol) with respect to the lowest energy one, taken as zero. Thus, the format "type_ΔE" (i.e., $\mathrm{b}'_{\mathrm{SB}}$_2.54 in the case of B3LYP/SBK(d) results) is used to discriminate among them. Since the lowest energy geometry of each diastereomer can differ depending on the computational method used, a number of low energy structures (ordered according to their stability at the B3LYP/SBK(d) level) are reported in Tables 1, 3 and 4, keeping similar arrangements on the same row. When comparing different structures, their numbering in Tables 1, 3 and 4 is also indicated ($1/\mathrm{b}'_{\mathrm{SB}}$_2.54). Furthermore, in the lower part of those tables, regio- and diastereoselectivity ratios determined from the reported values are displayed. High-energy structures, encountered in the systematic scan of each diastereomer TS degrees of freedom in an effort to elucidate the potential energy surface, however, have been disregarded because of their vanishingly small contribution to its population.

3.1. (1-vinyloxy-ethyl)-benzene (*1*)

The prevailing conformation (shown in Fig. 1(a)) of the most abundant diastereomer of the branched TS,

Table 1
Comparison among the relative stabilities (kcal/mol) obtained at the various levels for the alkyl-rhodium transition states of olefin **1**

Structure		B3P86/6-31G*	B3LYP/SBK(d)	B3P86/6-31+G*	B3P86/6-31G**
b		0	0	0	0
Reference energy[a]		−916.213153	−255.286431	−916.236828	−916.233012
b′	1	2.47	2.54	2.45	2.42
	2	3.15	2.90	3.23	3.11
	3	2.48	3.32	2.71	2.44
ℓ	switched C_{ap}	1.02	0.23	0.92	1.10
ℓ		1.42	0.68	1.41	1.48
ℓ'		1.94	1.47	2.02	1.98
Ratios					
b + b′:ℓ + ℓ'		89:11 [83:17] 77:23	72:28 [59:41] 49:51	89:11 [81:19] 75:25	90:10 [84:16] 79:21
ℓ:ℓ'		70:30 [82:18] 88:12	79:21 [89:11] 92:8	74:26 [86:14] 90:10	70:30 [82:18] 87:13
b:b′		96:4	97:3	97:3	96:4

[a] Hartrees.

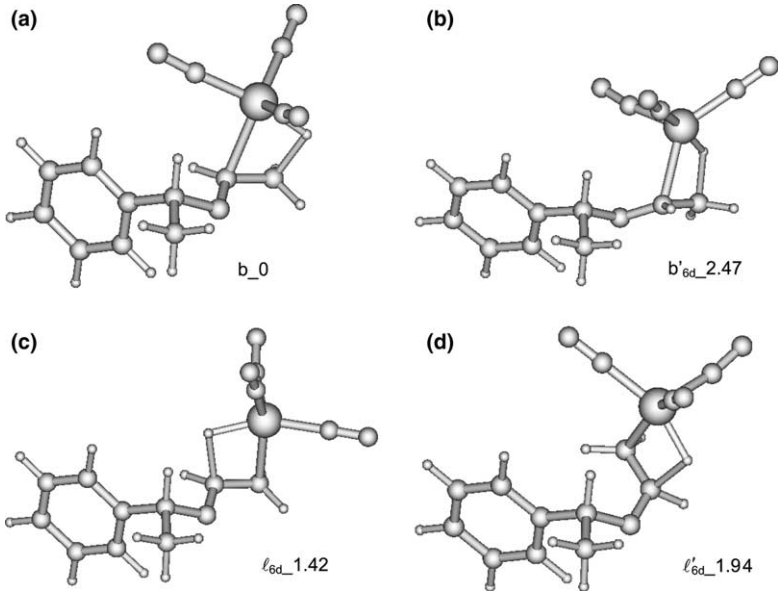

Fig. 1. Lowest energy structures for the various (R)-(1-vinyloxy-ethyl)-benzene···H–Rh(CO)$_3$ transition states: (a) b_0 (i.e., either 6d or SB), (b) b′$_{6d}$_2.47, (c) ℓ_{6d}_1.42, (d) ℓ'_{6d}_1.94.

b_0 (regardless method and basis set used, RR for the branched aldehyde product), is coplanar and *anti* ($164° < C_1C_2O_3C_4 < 168°$, depending on the method/basis set combination).[1] The H at C_2 (named H_2) is roughly parallel to the phenyl ring, with an $H_2\cdots C_5$ separation of 2.55–2.63 Å, while the O lone pairs point in opposite direction with respect to the phenyl ring, which is *gauche* ($60° < C_2O_3C_4C_5 < 63°$) to the vinyl group. Consequently, the methyl group is *trans* ($-177° < C_2O_3C_4C_7 < -173°$) to the vinyl group.

In general, B3LYP/SBK(d) geometries are fairly close to B3P86/6-31G* ones. Therefore only one structure is displayed in the figures for each diastereomer. The close agreement between B3LYP/SBK(d) and B3P86/6-31G* descriptions is observed indeed also for the most stable conformation of the less abundant diastereomer, b′ (RS for the branched aldehyde product), shown in Fig. 1(b), which is still coplanar, but remarkably differs from b because of the chirality change at C_2. Consequently, in this type of structure (which is less favorable than b by ~2.5 kcal/mol), the O lone pairs face the phenyl ring π distribution, while the methyl group faces H_2. The apical CO group is *trans* with respect to H_2 in both cases.

From the perusal of Table 1, the 6-31G* *syn* structure ($3/b'_{6d}$_2.48) has almost the same energy as $1/b'_{6d}$_2.47, while at the B3LYP/SBK(d) level ($3/b'_{SB}$_3.32) is less stable by about 0.8 kcal/mol than ($1/b'_{SB}$_2.54). Interestingly, a *syn* conformation ($C_1C_2O_3C_4$ close to −5°) also

[1] Atom numberings are displayed in Scheme 2. Geometrical parameters are reported in Table S4 (Supplementary Material).

prevails in the case of the isolated chiral vinyl ether (**1**), with the inner hydrogen of the terminal CH_2 facing the phenyl ring, whereas the *anti* conformation ($C_1C_2O_3C_4$ close to 176°) is significantly less favorable (by 1.00/1.17 kcal/mol) than the *syn* one [25] (data not shown). For TS with H–Rh(CO)$_3$ of **1** the trend is inverted only using B3LYP/SBK(d), while a substantial balance between *syn* and *anti* is obtained with B3P86/6-31G*.

As shown in Scheme 1, from antipodes with just one chiral center, a single enantiomer is obtained for linear aldehydes. However, as anticipated above, linear TS as well form a diastereomeric pair and, hence, it is advisable to discuss their stability in analogy with what done for the branched ones. Of course, no experimental data are available for ℓ and ℓ', but only for their sum, L. The most abundant linear diastereomer at the 6d and SB levels is ℓ, shown in Fig. 1(c), although there is a slightly different stability (1.42 and 0.68 kcal/mol, respectively) for closely related structures of *anti* type ($C_1C_2O_3C_4$ = 165.5° in both cases). The overall arrangement of the substrate is very similar to that found in the most stable branched diastereomer (Fig. 1(a)), apart obviously the H–Rh(CO)$_3$ way of attack, eventually leading to a linear aldehyde.

Interestingly enough, the ℓ' diastereomer (displayed in Fig. 1(d)) is *syn* ($C_1C_2O_3C_4 = -29.1°$ and $-28.4°$ at the 6d and SB levels, respectively). The substituents at the chiral center (C_4) are in a similar arrangement as in the case of b and ℓ: the phenyl ring is roughly *gauche* ($C_2O_3C_4C_5$ = 82.0° and 80.2°) to the vinyl group and the methyl group roughly *trans* ($C_2O_3C_4C_7 = -155.5°$ and $-157.6°$) to it. Therefore, in ℓ', the phenyl ring faces one of the hydrogens (H_1) of the vinyl terminal CH_2 group ($H_1\cdots C_5$ separation = 2.54 and 2.58 Å).

In both ℓ and ℓ' diastereomers, the phenyl π distribution and the ethereal O lone pairs point in opposite directions. This fact, associated with the co-planarity of main chain atoms, puts forward the principal difference between the two diastereomers in this case, i.e., the diverse steric interaction of the phenyl ring with the vinyl CH with respect to that of the phenyl itself with the vinyl CH_2. The apical CO group is on the same side of H_2 for all the L diastereomers, whereas it is on the opposite side with respect to H_2 in the branched ones. Nonetheless, only in the case of L diastereomers, switched stable TS exist as well, like ℓ_{SB}_0.23 (vide infra).

In almost all cases but one (2/b′), the H at C_4 points toward the same region of space where the attack of H–Rh(CO)$_3$ occurs, as expected from the steric hindrance of the bulky catalytic group. In the 2/b′ structures (not shown), however, the $C_2O_3C_4C_5$ dihedral is 82° and 71° and, although all the dihedral values are very close to those of the most stable transition state, the phenyl ring faces the catalytic group. This is due to the different diastereomeric structure of the two TS (b and b′). Albeit there is a significant energy penalty for structures with the phenyl ring close to the catalytic group,[2] at the B3LYP/SBK(d) level they can still contribute to the population. Thus it is not advisable to discard them a priori.

The stability depends on the mutual arrangement of the chiral group and the rhodium-vinyloxy moiety rather than on the other geometric parameters that are quite well conserved, with limited variations depending on the method/basis set used. The hydride being transferred is about at the same distance from Rh and the olefin carbon atom at the B3LYP/SBK(d) level, whereas at the B3P86 level the HC_n distance (with n = 1 or 2) is somewhat shorter than the HRh one: both separations are conversely larger in the case of linear TS as well as the C_1C_2 bond length (the latter especially in the case of *syn* structures). As an almost general feature, the B3LYP/SBK(d) values of bond lengths are significantly larger than the B3P86 one, apart some of those related to the rhodium complexation. The rhodium distance to the apical carbon atom (RhC_{ap}) is larger than that to the basal CO carbons (RhC_b), while the $C_{ap}O$ bond distance is slightly shorter than the C_bO ones. Nonetheless the difference in the RhC_{ap} and RhC_b separations is independent of the computational level and is about twice as much for the linear than for the branched alkyl rhodium TS (i.e., 0.9 vs 0.4 Å, respectively).

In order to investigate the stability of TS with either one of the equatorial CO groups moved to the apical position, a systematic search has been carried out, assigning to the proper C_b–O bond the C_{ap}–O bond length and vice versa. Thus OPT=TS optimizations have been performed while imposing such bond distance constraints (failure to do so invariably produced the original TS), eventually relieved once the structure had been optimized. This procedure allowed linear TS more favorable than those with the apical CO group *trans* with respect to H_2 to be located. Despite several trials, no stable switched TS were found along the path leading to the branched aldehydes.

To clarify the origin of the stability of linear TS at the B3LYP/SBK(d) level significantly larger than that obtained at the B3P86/6-31G* level, additional calculations with various descriptions have been carried out, whose results are reported in Tables 1 and 2. Interestingly, the addition to B3P86/6-31G* of either *sp* diffuse functions on main group atoms or of *p* polarization functions on H has a limited effect on the TS relative stability (last two columns of Table 1), without appreciable changes in the structures.

[2] Bond angles are slightly distorted to enhance the $H_2\cdots C_5$ separation to ~2.9 Å (with respect to a value of ~2.6 Å when otherwise oriented).

Table 2
Comparison among the relative stabilities (in kcal/mol) obtained at various levels for some alkyl-rhodium transition states of olefin **1**

Optimized structures			Single point calculations									
			B3P86/6-31G* TS geometry						TS geometry excluding H-Rh(CO)$_3$atoms			
									B3P86 6-31G*	B3LYP SBK(d)	B3P86 6-31G*	B3LYP SBK(d)
	B3P86 6-31G*	B3LYP 6-31G*	B3LYP SBK(d)	B3LYP Mix-BS1[c]	B3LYP Mix-BS2[d]	B3LYP SBK(d)	B3LYP Mix-BS1[e]	B3LYP Mix-BS3[f]	B3LYP Mix-BS4[g]	B3P86 6-31G*		B3LYP SBK(d)	
b	0	0[b]	0	0	0	0	0	0	0	0	0	0	0
Reference energy[a]	−916.213153	−913.611776	−255.286431	−914.236847	−314.530523	−255.278255	−914.235997	−492.264795	−677.250850	−464.908476	−464.890722	−79.615318	−79.617740
ℓ (C_{ap})	1.02	0.74	0.23	0.69	0.19	0.22	0.70	0.19	0.53	3.12	2.34	2.67	2.01
ℓ	1.42	1.24	0.68	1.11	0.64	0.66	1.12	0.64	1.02	3.62	2.84	3.07	2.44

[a] Reference energies in hartrees.
[b] Results obtained employing effective core potentials for Rh in the LANL2DZ valence basis set, with the other atoms described at the B3LYP/6-31G* level, i.e., using the LYP functional in place of the P86 one.
[c] Mix-BS1: Rh and H as in SBK(d) coupled to C and O atoms at the B3LYP/6-31G* level.
[d] Mix-BS2: Rh, C, non-ethereal O, and H as in SBK(d) with only the ethereal O at the B3LYP/6-31G* level.
[e] Basis set described in footnote (c).
[f] Mix-BS3: Rh, C, and H as in SBK(d) coupled to O at the B3LYP/6-31G* level.
[g] Mix-BS4: Rh, O, and H as in SBK(d) coupled to C at the B3LYP/6-31G* level.

The use of the LYP correlation functional in place of P86 somewhat reduces the gap between b and ℓ structures, apparent comparing the second to the first column in Table 2. An analogous gap is obtained replacing the SBK(d) description of all the C and O atoms in the complex with the B3LYP/6-31G* one (B3LYP/Mix-BS1, fourth column in Table 2), while no obvious correlation with natural [26] or Mulliken populations for those complexes can be found (see Figure S1 and Tables S7–S8). By substituting the ethereal O description only (B3LYP/Mix-BS2), the gap (fifth column) turns out to be even lower than the original one (third column).

In the right hand side of Table 2, results obtained with rigid geometries are compared. By using the B3P86/6-31G* geometries of three TS, the B3LYP/SBK(d) energy gaps (sixth column) are very close to the optimized ones (third column), in analogy with the behavior of the B3LYP/Mix-BS1 basis set (SBK(d) replaced with 6-31G* for all the C and O atoms), as can be seen by comparing the seventh column to the fourth one. Thus the gap enhancement is due to the B3LYP/6-31G* description of C and O atoms. By separately examining their effect, the main contribution is due to the C B3LYP/6-31G* description (ninth column) and to their mutual interaction, since the B3LYP/6-31G* description of O atoms alone (eighth column) slightly reduces the gap. Finally, excluding the contribution of the catalytic group, the structures leading to linear aldehydes are much less favorable than those leading to branched aldehydes. The LYP functional seemingly underestimates the gap, as already noted.

From the values reported in Table 1, diastereoselectivity (b:b′) ratios of 96:4 and 97:3 are obtained, which compare well with experimental diastereoselectivity (88:12) observed in hydroformylation reactions performed with $Rh_4(CO)_{12}$ as catalytic precursor in mild conditions [10b]. Concerning the regioselectivity ratios (B:L), due to the presence of a TS with a different arrangement of the catalytic group with respect to a single structure of the substrate, distinct choices are possible. Including only the linear TS with the apical group consistent with the other L regioisomers, regioselectivity ratios (at the left hand side in Table 1) of 89:11 and 72:28 are obtained, in satisfactory agreement with experimental regioselectivity (85:15) [10b]. Including the most stable linear TS only, disregarding its apical group orientation, regioselectivity ratios (within square brackets in Table 1) of 83:17 and 59:41 are obtained. In this case the B3P86/6-31G* ratio (83:17) is in excellent agreement with the experimental value, whereas the B3LYP/SBK(d) ratio (59:41) is too low, because of the B3LYP overestimate of the linear structure stability shown in Table 2. Including both linear TS, regioselectivity ratios (reported at the right hand side in Table 1) further decrease to 77:23 and 49:51. Conversely, ''vir-

tual'' stereoselectivity (ℓ:ℓ') ratios turn out to be 70:30 and 79:21. As expected, a variance in the ratio is observed depending on which diastereomers are included in the ℓ population.

3.2. (1-methyl-but-3-enyl)-benzene (2)

When in the chiral olefin the ethereal oxygen is replaced with a methylene group[3] as occurs in (1-methyl-but-3-enyl)-benzene (**2**), the conformational freedom of the main chain,[4] $C_1C_2C_3C_4$ (atom numbering in Scheme 2), is much higher than in **1**. This fact allows a good number of low energy transition states to be located, as can be inferred from the wealth of structures reported in Table 3. In contrast to **1** (where only *syn* and *anti* structures were obtained), several *gauche*+/*gauche* − TS, in which the steric repulsion between catalytic groups and bulky substituents at the chiral carbon (C_4) is relieved, have been found for **2** beside *cis* and *trans* arrangements. It is noteworthy that the few local minima of *cis* structure obtained are somewhat higher in energy (2.6, 2.9 kcal/mol and 2.2, 2.4 kcal/mol above the lowest minimum for b′ and ℓ', respectively) than *gauche* and *trans* structures: whether *gauche* or *trans* prevails depends on the configuration type and, to a lesser extent, on method/basis set.

In contrast, in the isolated substrate **2**, *gauche* conformations ($C_1C_2C_3C_4 = -120.4°, -120.3°$) have been obtained starting from *trans* conformations in all cases. They are more favorable by ~1.1, 1.6 kcal/mol than the *cis* ones ($C_1C_2C_3C_4 = -0.9°, 0.3°$) with a *gauche:cis* population of 87:13, 94:6, respectively, while no local minimum of *trans* type has been located.

For this substrate, the most stable TS configurations can be of b and ℓ type without any preference for either one: at the B3LYP/SBK(d) level they have exactly the same energy, while at the B3P86/6-31G* level the (b − ℓ) energy gap is only 0.22 kcal/mol. The most stable TS configurations of b′ and ℓ' type are just slightly less stable than the previous two types. The (b − b′) and ($\ell - \ell'$) energy gaps are −0.17, −0.21 and −0.45, −0.24 kcal/mol, respectively.

The structures for b and b′ are *gauche* with the phenyl ring facing C_1 (Fig. 2(a)) or H_2 (Fig. 2(b)), as can be derived also from the data reported in Supplementary Material (Table S5). The apical CO groups in Figs. 2(a) and (b) point downward. An almost *trans* arrangement of the aliphatic backbone, with the phenyl ring roughly perpendicular to it, has been found for the most stable ℓ TS configurations, all as favorable as b (or even more favorable at the B3P86/6-31G* level), displayed in Fig. 2(c) ($C_1C_2C_3C_4 = 154.3°, 159.6°$). In contrast, the most stable ℓ' configurations (shown in Fig. 2(d)), with an arrangement very similar to that of b′ (see Fig. 2(b), where $C_1C_2C_3C_4 = 89.6°$ and 88.3°, respectively at the B3P86/6-31G* and B3LYP/SBK(d) levels), are *gauche* ($C_1C_2C_3C_4 = 87.9°, 88.3°$). This fact indicates that *gauche* conformations are easily reachable in substrate **2** as in the isolated molecule. The substrate structures are well conserved in b and ℓ (compare Fig. 2(a) with (c)) as well as in b′ and ℓ' (compare Fig. 2(b) with (d)) regardless the different points of attack of H–Rh(CO)$_3$, that produce no change in the former case or a very limited change in energy (0.06, 0.03 kcal/mol) in the latter case, much lower than that computed for **1** (1.4, 0.7 kcal/mol) where only b and ℓ can be compared.

Table 3
Comparison among the relative stabilities for the alkyl-rhodium transition states of olefin **2**

Structure		B3P86/6-31G*	B3LYP/SBK(d)
b	1	0.22	0[b]
	2	0.46	0.42
b′	1	0.39	0.21
	2	1.20	0.88
	3	1.10	1.00
	4	1.42	1.38
ℓ	1	0[a]	0[b]
	2	0.82	0.69
	3	1.37	0.86
	4	1.75	1.89
	5	3.45	3.02
ℓ'	1	0.45	0.24
	2	1.00	0.94
	3	1.50	1.23
	4	1.92	1.39
	5	2.18	2.24
	6	2.20	2.38
	7	3.04	2.97
Ratios			
b + b′:ℓ + ℓ'		48:52	50:50
b:b′		56:44	55:45

[a] Reference energy −880.320640 hartrees.
[b] Reference energy −246.170654 hartrees.

For substrate **2** the computational level does not significantly affect the results. However, the B3P86/6-31G* results are even closer to the B3LYP/SBK(d) ones than for substrate 1.

In order to clarify the main differences between **2** and **1**, it is noteworthy that in *trans* structures the phenyl ring is much skewer to the ethereal backbone than to the hydrocarbon one. Moreover, beside *trans* arrangements, substrate **1** can take *syn* structures, while substrate **2** can assume less hindered *gauche* geometries, due to the greater flexibility of its backbone. This allows the $H_1\cdots C_5$ distance, as a measure of the phenyl ring-terminal CH_2 group separation, take values larger than 3 Å (b_{6d}_0.2 shown in Fig. 2(a)) whereas it is just 2.54 Å in **1** (ℓ'_{6d}_1.94 shown in Fig. 1(d)). Thus, a fairly large

[3] As already put forward, due to the priority rules, an S configuration has been used for substrate **2** in order to keep the substituents in the same mutual position as in substrate **1**.
[4] Geometrical values are reported in Table S5.

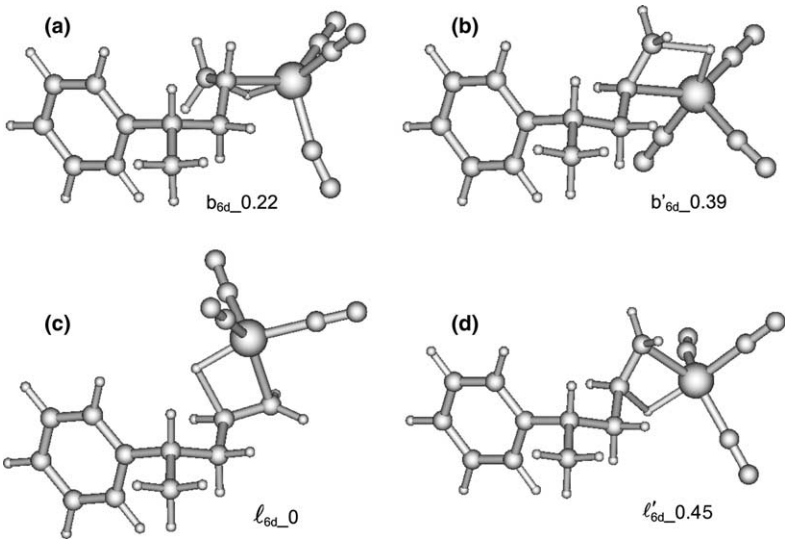

Fig. 2. Lowest energy structures for the (S)-(1-methyl-but-3-enyl)-benzene···H–Rh $(CO)_3$ transition states: (a) b_{6d}_0.22, (b) b'_{6d}_0.39, (c) ℓ_{6d}_0, (d) ℓ'_{6d}_0.45.

separation between the substituents at the chiral center and the vinyl group coordinated to H–$Rh(CO)_3$ is found in substrate **2**, due to the hydrocarbon chain flexibility and to the almost free rotation around the CH_2 group, in contrast to what happens in the presence of the ethereal oxygen. This fact allows the catalyst to attack the less hindered face as observed in our recent theoretical studies carried out on a different kind of catalyzed reaction [27].

The geometric features of the olefin-catalytic group complex show some regularity within each computational level. From a perusal of the rows in Table S5 related to bond distances and angles, in the attack region there are close similarities in the values obtained for branched and linear diastereomers, in contrast to what found for **1** (Table S4), which is reflected in the remarkably different stabilities as well. In particular, the flexibility of substrate **2** is put forward by the significant change in the $RhC_2C_3C_4$ torsion depending on the value assumed by the $C_1C_2C_3C_4$ dihedral: when $C_1C_2C_3C_4$ is *gauche*, $RhC_2C_3C_4$ is *trans* and vice versa. On the contrary, for substrate **1**, even when $C_1C_2O_3C_4$ is *syn*, $RhC_2O_3C_4$ is *gauche* and, for ℓ' diastereomers, *syn* $C_1C_2O_3C_4$ values (−29.1°, −28.4°) correspond to *syn* $RhC_2O_3C_4$ values (44.6°, 46.3°). No couples of structures with switched C_{ap} have been found for substrate **2**.

Therefore, regio- and diastereoselectivity ratios close to 50:50 are foreseeable. From the values reported in Table 3, a regioselectivity (B:L) of 48:52 and 50:50 and a diastereoselectivity (b:b′) of 56:44 and 55:45, are obtained indeed. The corresponding experimental values are 49:51 and 52:48, respectively [10b]. Taking into account that values close to 50:50 are very sensitive to even very small energy differences, the agreement is almost perfect. Confident that the method is possibly viable for predictions, the study has been extended to a chiral substrate not yet employed for hydroformylation reactions with unmodified rhodium catalysts under mild conditions.

3.3. (1-methyl-allyl)-benzene (3)

The chiral group is S, as in **2**, to allow a direct comparison between the substituents kept in similar mutual positions. In this case the chiral C atom is directly bonded to the C involved in the double bond, in contrast with the substrates previously considered (**1** and **2**). Thus the absence of a separator keeps the catalytic and chiral groups very close to each other. In principle, this fact could impose a large steric hindrance, affecting the transition state stability. However, the rotational capabilities of an sp^3 carbon atom might relieve the structure strain. Actually, the conformations of the main chain,[5] $C_1C_2C_3C_4$, are close to those obtained for substrate **2**. As displayed in Fig. 3, the b and ℓ lowest energy configurations of the TS of substrate **3** are *gauche*, while the b′ and ℓ ones are *trans*. Of course, in turn, the adjacent methyl group is *trans* in the former cases and *gauche* in the latter ones.

Among the computational levels considered there is a limited consensus about ℓ' as the most stable configuration, although the stability of the various configurations are fairly comparable. Apart the arrangement of the catalytic group, the b and ℓ configurations as well as the b′ and ℓ' ones are very similar to each other, as apparent from Fig. 3. The phenyl ring torsion about the C_3C_4 bond is only slightly affected by the vicinity of the bulky Rh carbonyl moiety in b′ and ℓ'.

[5] Atom numbering in Scheme 2. Some geometrical parameters are reported in Table S6.

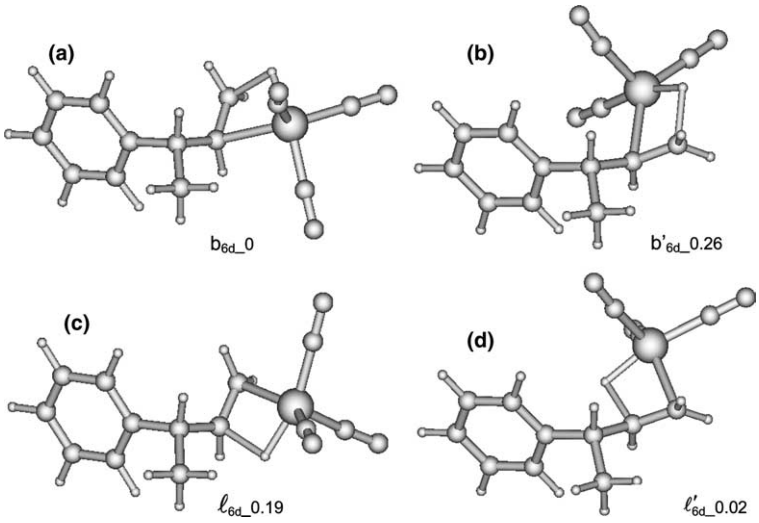

Fig. 3. Lowest energy structures for the (S)-(1-methyl-allyl)-benzene···H–Rh(CO)$_3$ transition states: (a) b_{6d}_0, (b) $b'_{6d}\_0.26$, (c) $\ell_{6d}\_0.19$, (d) $\ell'_{6d}\_0.02$.

Table 4
Comparison among the relative stabilities obtained at the various levels for the alkyl-rhodium transition states of olefin **3**

Structure		B3P86/6-31G*	B3LYP/SBK(d)
b	1	0[a]	0.06
	2	1.73	2.24
	3	2.33	2.98
b′	1	0.26	0.42
	2	1.14	1.48
	3	1.69	2.52
ℓ	1	0.19	0.28
	2	1.04	1.68
	3	1.62	1.86
ℓ'	1	0.02	0[b]
	2	0.66	1.01
	3	0.93	1.57
Ratios			
b + b′: ℓ + ℓ'		44:56	44:56
b:b′		56:44	61:39

[a] Reference energy −840.858990 hartrees.
[b] Reference energy −239.314912 hartrees.

The additional minimum energy structures obtained for the branched TS of substrate **3**, reported in Table 4, are decidedly less favorable than the most stable ones: therefore, their exclusion from the calculation of the b:b′ diastereoselectivity ratio would just enhance its value to 61:39 (from 56:44) at the B3P86/6-31G* level and to 65:35 (from 61:39) at the B3LYP/SBK(d) one. Conversely, the exclusion of the additional linear regioisomers would significantly affect the ratios.

In summary, the picture of regioselectivity for the reaction involving substrate **3** is well conserved (44:56 in both cases), while there is agreement concerning stereoselectivity (56:44 and 61:39 at the B3P86/6-31G* and B3LYP/SBK(d) levels, respectively). Interestingly, when the b:b′ diastereoselectivity is low, also the "virtual" ℓ:ℓ' diastereoselectivity is modest (39:61 and 37:63 at the B3P86/6-31G* and B3LYP/SBK(d) levels, respectively), as can be derived from the data in Table 4.

4. Conclusions

The sensitivity to method and basis set of transition states in the hydroformylation reaction of chiral substrates (a vinylether and two olefins), using an unmodified rhodium carbonyl catalyst such as H–Rh(CO)$_3$, was investigated with two DFT functionals (B3P86 and B3LYP). TS stabilities and structures were taken into account with the 6-31G* basis set (including effective core potentials for Rh in the LANL2DZ related valence basis set) at the B3P86 level, while the SBK(d) basis set, making use of effective core potentials for Rh and main group atoms (for its description refer to the Computational Details section) was used at the B3LYP level. The main problem in the conformational analysis of this kind of systems is the great number of conformers per each configuration to be considered, due to the difficulty in locating all low energy transition states, on which regio- and stereomeric ratios depend. CO group arrangements as well deserve attention in order to take into account all distinct conformers. Missing low energy structures are actually the principal source of error in computed ratios.

In the case of substrate **1** ((1-vinyloxy-ethyl)-benzene), B3P86/6-31G* and B3LYP/SBK(d) favor *anti* arrangements, although few *syn* structures can be located. As a common feature, B3LYP/SBK(d) stability values are close to the B3P86/6-31G* ones. Geometrical parameters as well are fairly comparable despite the different combinations of level/basis set used. The B3LYP description seemingly overestimates the stability of transition states leading to linear aldehydes. No particular

improvement in the results is found employing additional *sp* diffuse functions on C and O atoms or polarization functions on H atoms.

In the case of substrate **2** ((1-methyl-but-3-enyl)-benzene), a conformational flexibility significantly larger than in **1** is obtained, due to the CH_2 group replacing the ethereal oxygen. Therefore, in addition to *trans* structures of the $C_1C_2C_3C_4$ backbone, several *gauche* arrangements were located, that reduce the steric hindrance between the bulky (catalytic and chiral) groups present in the TS. This fact prevents any chiral discrimination for this substrate: the b:b′ diastereoselectivity ratio is well balanced because *gauche* structures have been obtained for b and b′.

In the case of substrate **3** ((1-methyl-allyl)-benzene), chiral and catalytic groups are very close to each other, because of the lack of a separator (either O or CH_2). Despite the vicinity of those bulky groups, the flexibility of the backbone is still similar as that obtained for substrate **2**. Furthermore, the regioselectivity (44:56) is strictly maintained. As far as diastereoselectivity is concerned, both descriptions are fairly consistent.

The agreement of the computed results with experimental data obtained under mild experimental condition is good especially at the B3P86/6-31G* level: its use should thus be recommended. This approach might eventually lead to the rational design of substrates with the aim of obtaining specific marketable products.

Acknowledgement

We are indebted to R. Lazzaroni for introducing us into the field of Rh-catalyzed hydroformylation reactions.

Appendix A. Supplementary data

Supplementary data associated with this article can be found, in the online version, at doi:10.1016/j.jorganchem.2004.12.038.

References

[1] (a) B. Cornils, W.A. HerrmannApplied Homogeneous Catalysis with Organometallic Compounds, vol. 1, VCH-Wiley, New York, 1996, pp. 3–25;
(b) G. Papadogianakis, R.A. Sheldon, New J. Chem. 20 (1996) 175;
(c) M. Beller, B. Cornils, C.D. Frohning, C.W. Kohlpaintner, J. Mol. Catal. A 104 (1995) 17;
(d) G.W. Parshall, S.D. Ittel, Homogeneous catalysis, second ed., Wiley, New York, 1992.

[2] (a) J.P. Collman, L.S. Hegedus, J.R. Norton, R.G. Finke, Principles and applications of organotransition metal chemistry, University Science Books, Mill Valley, 1987;
(b) R.H. Crabtree, The Organometallic Chemistry of the Transition Metals, Wiley, New York, 1988.

[3] O. Roelen, (Ruhrchemie AG) DBP 849 (1938) 458; Chem. Zentr. (1953) 927.

[4] (a) G. Süss-Fink, G. Meister, Adv. Organomet. Chem. 35 (1993) 41;
(b) F. Ungváry, Coord. Chem. Rev. 167 (1997) 233;
(c) F. Ungváry, Coord. Chem. Rev. 170 (1998) 245;
(d) F. Ungváry, Coord. Chem. Rev. 188 (1999) 263.

[5] (a) M. Torrent, M. Solà, G. Frenking, Chem. Rev. 100 (2000) 439, and references therein;
(b) S.A. Decker, T.R. Cundari, Organometallics 20 (2001) 2827;
(c) S.A. Decker, T.R. Cundari, J. Organomet. Chem. 635 (2001) 132;
(d) D. Gleich, J. Hutter, Chem. Eur. J. 10 (2004) 2435.

[6] (a) I. Wender, P. Pino, Organic Syntheses via Metal Carbonyls, vol. 2, Wiley-Interscience, New York, 1977;
(b) J. Falbe, New syntheses with carbon monoxide, Springer, Berlin, 1980.

[7] F. Agbossou, J.-F. Carpentier, A. Montreaux, Chem. Rev. 95 (1995) 2485.

[8] (a) D. Evans, J.A. Osborn, G. Wilkinson, J. Chem. Soc. A (1968) 3133;
(b) S. Gladiali, J.C. Bayón, C. Claver, Tetrahedron: Asymm. 6 (1995) 1453;
(c) N. Sakai, S. Mano, K. Nozaki, H. Takaya, J. Am. Chem. Soc. 115 (1993) 7033.

[9] (a) M. Tonti, Regio- and diastereoselectivity in the rhodium-catalyzed hydroformylation of chiral arylalkylvinylethers. Thesis, University of Pisa, 1998–1999;
(b) R. Lazzaroni, S. Bertozzi, P. Pocai, F. Troiani, P. Salvadori, J. Organomet. Chem. 295 (1985) 371;
(c) R. Lazzaroni, S. Pucci, S. Bertozzi, J. Organomet. Chem. 247 (1983) C56;
(d) I. Amer, H. Alper, J. Am. Chem. Soc. 112 (1990) 3674;
(e) M.P. Doyle, M.S. Shanklin, M.V. Zlokazov, Synletter (1994) 615.

[10] (a) G. Alagona, C. Ghio, R. Lazzaroni, R. Settambolo, Organometallics 20 (2001) 5394;
(b) G. Alagona, C. Ghio, R. Lazzaroni, R. Settambolo, Inorg. Chim. Acta 357 (2004) 2980.

[11] M.J. Frisch, G.W. Trucks, H.B. Schlegel, G.E. Scuseria, M.A. Robb, J.R. Cheeseman, V.G. Zakrzewski, J.A. Montgomery, R.E. Stratmann, J.C. Burant, S. Dapprich, J.M. Millam, A.D. Daniels, K.N. Kudin, M.C. Strain, O. Farkas, J. Tomasi, V. Barone, M. Cossi, R. Cammi, B. Mennucci, C. Pomelli, C. Adamo, S. Clifford, J. Ochterski, G.A. Petersson, P.Y. Ayala, Q. Cui, K. Morokuma, D.K. Malick, A.D. Rabuck, K. Raghavachari, J.B. Foresman, J. Cioslowski, J.V. Ortiz, B.B. Stefanov, G. Liu, A. Liashenko, P. Piskorz, I. Komaromi, R. Gomperts, R.L. Martin, D.J. Fox, T. Keith, M.A. Al-Laham, C.Y. Peng, A. Nanayakkara, C. Gonzalez, M. Challacombe, P.M.W. Gill, B.G. Johnson, W. Chen, M.W. Wong, J.L. Andres, M. Head-Gordon, E.S. Replogle, J.A. Pople, Gaussian 98 (Revision A6), Gaussian Inc, Pittsburgh, PA, 1998.

[12] A.D. Becke, J. Chem. Phys. 98 (1993) 5648.

[13] (a) J.P. Perdew, Phys. Rev. B 33 (1986) 8822;
(b) J.P. Perdew, Phys. Rev. B 34 (1986) 7406.

[14] J.S. Binkley, J.A. Pople, W.J. Hehre, J. Am. Chem. Soc. 102 (1980) 939.

[15] (a) R. Ditchfield, W.J. Hehre, J.A. Pople, J. Chem. Phys. 56 (1972) 2257;
(b) P.C. Hariharan, J.A. Pople, Theor. Chim. Acta 28 (1973) 213.

[16] (a) T.H. Dunning Jr., P.J. Hay, in: H.F. SchaeferIII (Ed.), Modern Theoretical Chemistry, Plenum, New York, 1976, pp. 1–28;
(b) P.J. Hay, W.R. Wadt, J. Chem. Phys. 82 (1985) 270;
(c) P.J. Hay, W.R. Wadt, J. Chem. Phys. 82 (1985) 299.

[17] C. Lee, W. Yang, R.G. Parr, Phys. Rev. B 37 (1988) 785.

[18] (a) W.J. Stevens, H. Basch, M. Krauss, J. Chem. Phys. 81 (1984) 6026;

(b) W.J. Stevens, H. Basch, M. Krauss, P. Jasien, Can. J. Chem. 70 (1992) 612;
(c) T.R. Cundari, W.J. Stevens, J. Chem. Phys. 98 (1993) 5555.
[19] S. Huzinaga, J. Andzelm, M. Klobukowski, E. Radzio-Andzelm, Y. Sakai, H. Tatewaki, Gaussian Basis Sets for Molecular Calculations, Elsevier, Amsterdam, 1984.
[20] R. Ditchfield, W.J. Hehre, J.A. Pople, J. Chem. Phys. 54 (1971) 724.
[21] R. Lazzaroni, G. Uccello-Barretta, M. Benetti, Organometallics 8 (1989) 2323.
[22] C.P. Casey, L.M. Petrovich, J. Am. Chem. Soc. 117 (1995) 6007.
[23] D. Gleich, R. Schmid, W.A. Herrmann, Organometallics 17 (1998) 4828.
[24] (a) N. Koga, S.Q. Jin, K. Morokuma, J. Am. Chem. Soc. 110 (1988) 3417;
(b) T. Matsubara, N. Koga, Y. Ding, D.G. Musae, K. Morokuma, Organometallics 16 (1997) 1065.
[25] Even in the case of methyl vinyl ether, the cis form is the most stable at room temperature, while the trans form appears at higher temperature, as demonstrated since long with spectroscopic studies by N.L. Owen, N. Shepherd, Trans. Farad. Soc. 60 (1964) 634.
[26] NBO (version 4.0) E.D. Glendening, A.E. Reed, J.E. Carpenter, F. Weinhold, Theor. Chem. Inst., University of Wisconsin, Madison, 1996.
[27] (a) G. Alagona, C. Ghio, M. Persico, S. Tomasi, J. Am. Chem. Soc. 125 (2003) 10027;
(b) G. Alagona, C. Ghio, S. Tomasi, Theor. Chem. Acc. 111 (2004) 287.